 DOE-ER-04721-4

EXPERIMENTAL NUCLEAR AND RADIOCHEMISTRY

Progress Report

for Period February 1, 1980 - January 31, 1981

Paul J. Karol

Department of Chemistry
Carnegie-Mellon University
Pittsburgh, PA 15213

November 1980

Prepared for the U. S. Department of Energy Under
Contract No. DE-AS02-78ER04721

DISCLAIMER

EXPERIMENTAL NUCLEAR AND RADIOCHEMISTRY

Abstract

"Experimental Nuclear and Radiochemistry" entails the investigation of deep nuclear spallation reactions induced by high-energy light particles on complex nuclei. Experimental studies involve activation of various medium to heavy mass targets bombarded by pi-mesons, protons and alpha particles. A prime objective is to deconvolve the cascade and evaporation steps in the reaction mechanism. Experimentally, particular emphasis has been placed on spallation products far from yield maxima where the deconvolution is most justifiable. Irradiations have been performed predominantly at the Clinton P. Anderson Los Alamos Meson Physics Facility. Results of cross section determinations from bombardments of ^{89}Y, ^{92}Mo, ^{96}Mo and ^{100}Mo with 800 MeV protons have nearly been completed, providing comparison of isobaric and mass-yield distributions. Data have also been obtained at 500 MeV. Theoretical efforts are being directed at the evaporative behavior of very high-temperature nuclei as determined by the nuclear equation of state and how such behavior might be observed in very deep spallation processes. In addition, the "soft spheres" model has been combined with spallation systematics to explore the feasibility of high-intensity beams to incinerate high-level nuclear wastes and also to predict interaction lengths in nuclear emulsion studies of relativistic heavy ions.

Table of Contents

Isobaric-Yield Distribution Functions

We have continued to explore ways in which isobaric yield distributions can be expressed mathematically such that a minimum of uncertainty is introduced in their construction or reconstruction from data and yet they reflect physically significant information. The conventional distribution form has been a symmetric one such as the gaussian introduced by Rudstam.[1] Porile[2] used a form varying as

$$\exp[\alpha_5 + \alpha_6 A + \alpha_7 A^2][Z_p - Z]^{\alpha_8} \qquad (1)$$

Cumming,[3] recognizing that the distributions are asymmetric used a gaussian with a smoothly joined exponential tail. Ku and Karol[4] employed a skewed gaussian. Last year, our group found that the gaussian skewing polynomial goes unphysically negative at the distribution extremities. To remedy this situation we found that proper mathematical and physical behavior was possible if the skewing function were the complementary error function, that is

$$\sigma(x) = A(2\pi)^{-1/2} \exp[-x^2/2] \operatorname{erfc}[x + \zeta] \qquad (2)$$

where ζ serves as the skewing parameter.

An additional facet of this problem lies in the choice of the compositional variable "x" in the above expression and also the distribution functions chosen by others. Many groups, as in eq. (1) above, use "x" to mean Z_p-Z or distance from the peak, Z_p, in units of charge. In such cases, adjustments to cross section data from many mass chains have been made according to the Z_A-Z value or distance from the most stable isobar in units of nuclear charge. An alternate choice has been to use "x" to mean $(N/Z) - (N/Z)_p$, or neutron-to-proton ratio. We have used this in the past because we felt that N/Z was a

variable more suited to reflecting the changing width of the mass-energy valley as a function of A. Use of N/Z can be misleading, though. For example, a graph of masses for the A = 100 isobar against both Z and N/Z in Fig. 1 shows the expected symmetric parabolic form against Z but a decidedly asymmetric distribution in terms of N/Z.

Our original rationale for employing N/Z as the appropriate variable was recognition that the residual spallation isobaric yield distribution was influenced to a considerable degree by the width of the stability valley. This dependence must be accounted for in constructing isobaric yield distributions from a sometimes wide range of masses by interpolation and shifting. Using $Z-Z_A$ does not accomplish this but $(Z-Z_A)/\sigma_m$, there σ_m is an appropriately chosen stability valley width, should be suited to the task. Another way of expressing this point follows. If all yields were truly obtained at the same mass one would directly have the correct distribution. However, when using a yield from, for example, a higher mass than the one of interest, a correction is needed not only for the yield but also for the greater breadth of the stability valley at the higher mass. It is erroneous to employ just distance from valley minimum as the variable.

We have chosen to quantify our σ_m as follows. The width of the stability valley shall be measured at a fixed height, H (in energy or mass units), as a function of mass. Myer's droplet model[5] masses without shell corrections were fitted to a quadratic polynomial at several masses and the best values for a and b were obtained for

$$M(Z,A) = a_A Z^2 + b_A Z + c_A \qquad (3)$$

The fixed height above the valley is given by

$$H \equiv M(Z,A) - M(Z_A) = a_A Z^2 + b_A Z + \frac{b_A^2}{4a_A} \qquad (4)$$

and the most stable isobar is given by

$$Z_A = -b_A/2a_A \qquad (5)$$

Equations (3) and (4) can be arranged to give

$$|Z-Z_A| = |\sqrt{H/a_A}|$$

Since H is arbitrary, the valley width at constant depth, σ_m is proportional to $|a_A|^{-1/2}$. The droplet model gives a_A as a function of A which, when fitted to a simple power law, gives

$$\sigma_m \propto A^{0.44}$$

which is what we chose to employ until further refinements are made.

Noteworthy comparisons to existing analyses can be made. Our σ_m is similar to a standard deviation. Rudstam's R-parameter is explicitly related to standard deviation by $\sigma = (2/R)^{1/2}$. From Porile's recent work on Ag[2] spallation one obtains $\sigma \simeq 0.23\ A^{0.39}$ and from Kaufman's recent analysis of Au spallation[6] one obtains $\sigma \simeq 0.26\ A^{0.40}$. The agreement with our proposed parametrization is encouraging. Also, in his review of statistical evaporation from highly excited nuclei, LeCouteur[7] had calculated not only the displacement of the average product from stability but also the dispersion of the evaporation distribution. We fitted LeCouteur's results again to a power law, and obtained $\sigma \simeq 0.116\ A^{0.49}$. The A-dependence is in excellent agreement with experiment and our suggested quantification.

As a consequence of these arguments we are proceeding to treat all data,

our own and others according to Eq. (2) in which we will define x as

$$x = f(A) \equiv \frac{Z-Z_A}{A^{0.44}}$$

Experimental Isobaric Yield Distributions

During the past year, seven bombardments at 500 MeV were performed and sixteen at 800 MeV using the Area B proton beam line at Los Alamos. In most cases, rapid chemical separations were employed following transport of the target from the beam line to the nuclear chemistry laboratory using the pneumatic transport system. The experimental group this year was able to operate the complex transport system unassisted by LAMPF personnel and, in fact, provided valuable assistance in trouble-shooting for subsequent users.

Our results to date have been analyzed to provide relative isobaric yield curves in a few selected mass regions as a function of target composition and bombardment energy. These are presented on the following pages as Figures 2 through 7. From the isobaric yield curves and additional production yields in other mass regions, the mass-yield curve shown in Fig. 8 can be constructed. The logarithmic slope of the mass-yield curve is viewed as a nuclear thermometer, being indicative of average deposition energy following the cascade step. Table I lists the thermometric slopes we have determined. The only attempted quantification between the logarithmic slope and cascade deposition energy was made by Rudstam whose analysis of spallation yield systematics in 1966 gives a logarithmic slope of (12.9 $\pm$ 5.9)% per amu at 800 MeV. Rudstam recognized that this slope is a measure of nucleons removed which in turn correlates very strongly with excitation energy. No rigorous quantification has been attempted to date, however.

Eventually, in using our results to infer something about the behavior of high-temperature nuclei, an important step is confirmation of our most

critical assumption: that spallation isobars observed away from the stability valley have been formed by evaporation from a fairly restricted range of cascade product N, Z and E^*. The spallation yield results we obtained this year have strongly indicated this hypothesis is correct. Part of our justification for this conclusion is our observation from INC calculations of the excitation energy distributions following cascades of varying chain lengths. That is, in order to form final spallation products at large ΔA, you can have a very short cascade chain which deposits a large E^* followed by a long evaporation chain, or a long cascade chain depositing little E^* so that the subsequent evaporation sequence involves few particles, if any. Since E^* varies with cascade chain length, neither of the above extreme scenarios pertains. The correct combination is distributed in between and can be located by INC-evaporation calculation, insofar as these are reasonably modelled.

As an illustration, we can approximate the dependence of $\bar{E}^*$ on $\Delta A_{cascade}$ as a direct one with proportionality constant $c \sim 30$ MeV: $\bar{E}^* = c\Delta A_{casc}$. The length of the subsequent evaporation chain, ΔA_{evap}, is related to $\bar{E}^*$ through $\varepsilon \sim 12$ MeV, the average energy removed per evaporated particle: $\Delta A_{evap} = \bar{E}^*/\varepsilon$. INC calculations provide c and evaporation calculations yield values for ε. From these values, this simplified illustration shows that $\bar{E}^*$ is related to the total mass difference ΔA between target and measured product by

$$\bar{E}^* = \Delta A[(c\varepsilon)/(c+\varepsilon)] \tag{6}$$

where ΔA, of course, is also $\Delta A_{casc} + \Delta A_{evap}$. Hence

$$\Delta A_{casc} = \Delta A[\varepsilon/(c+\varepsilon)] \tag{7}$$

and

$$\Delta A_{evap} = \Delta A[c/(c+\varepsilon)] \tag{8}$$

The actual calculations show the two relationships between ΔA_{casc} and $\bar{E}^*$ and ΔA_{evap} and $\bar{E}^*$ to be somewhat more complicated than this illustration but the conclusion remains unchanged. Observing spallation products at a given "depth" ΔA inherently limits the ranges of the contributing cascade and evaporation chains. For $\Delta A = 30$, our simplified illustration gives $\bar{E}^* \sim 260$ MeV and $\Delta A_{casc} \sim 9$. Experimentally, this is reflected in the unchanged isobaric yield distributions for deep spallation at different bombarement energies for the several distinct systems we have analyzed this year. See Figure 9.

The crucial extension of this argument is that by examining very deep spallation we are necessarily viewing evaporative de-excitation from nuclei at high temperatures. Furthermore, we know roughly at what temperatures these hot nuclei must have started and their approximate identities if we confine ourselves to the wings of the isobaric yield distributions.

Most of the cross sections for spallation of the medium mass targets ^{89}Y, ^{92}Mo, ^{96}Mo and ^{100}Mo have now been determined. An integral component of our proposal is the necessary examination of heavier target regions as well. We have begun irradiations of ^{130}Te and ^{209}Bi for this purpose. Spallation cross sections from 800 MeV protons incident on ^{130}Te are listed in Table II for those products already analyzed. Even for $\Delta A \sim 50$, the yields appear appreciable which is very encouraging.

Density Depletion in Deep Spallation

Of prime concern in recent years, especially in conjunction with relativistic heavy ion (RHI) interactions, has been the question of the behavior of nuclear matter at high density. The nuclear equation of state

predicts what thermodynamics and even kinetics pertain, but the equation of state is model dependent. The question of the existence or non-existence of density isomers is an objective of RHI research. The abrasion-ablation model also indirectly involves similar input in the sense that part of the excitation energy results from a distortion of the residue from its equilibrium shape.

Part of our overall objective is to explore the high temperature nuclear equation of state. Production of high-temperature nuclei is accomplished by multiple nucleon-knockout via a light heavy ion induced cascade. We have examined intranuclear cascade (INC) calculations by Kaufman[8] for 1 GeV protons incident upon Au. Shown in Fig. 10 is a plot of residual excitation energy as a function of residue N/Z for cascades in which $\Delta A = 15$ and 16 and shows, for example, that excitation E^* is correlated to a degree with cascade path on the (N,Z) surface. Figure 11 shows that high excitation residues are strongly associated with small impact parameters. In Fig. 12 the correlation between E^* and ΔA is illustrated. High excitation can generally be associated with knockout of many nucleons from a projectile-target collision at small impact parameter. The cascade residue is left not only with high thermal excitation but also with a density reduced from its equilibrium value due to fast nucleon removal. Internal potential energy is associated with this density depletion. Upon relaxation, energy released by "contraction" is also available for nucleon evaporation. Our preliminary estimates are that this available energy, ignored in current statistical evaporation calculations, can amount to many tens of MeV and is most important at high excitation energy. We have also continued to examine the effect of depleted density on two other ignored aspects of the theory of nuclear

evaporation. These are the effects on level densities and on the location of the perceived valley of stability. Each of these facets is proving to be influential in high-temperature evaporation.

Neutron Deficient Nuclides

Nuclei which lie near the N = Z line with A > 60 are anticipated to provide stringent tests for theories of mass-energy. The situation is complicated by conflicting data. For example, the Table of Isotopes[9] lists a 5 m ^{84}Zr as opposed to the 26 m ^{84}Zr we see, an 8 m ^{79}Sr which we should have seen but didn't is apparently a 2.3 m isotope.[10] The nuclide ^{78}Sr has been reported with an anomalously large 31 m half-life. Its yield from production by spallation of ^{89}Y or ^{92}Mo should be sufficient for us to have seen the isotope with ease, yet we do not. ^{78}Rb^{m+g} are seen, but the yield remains undetermined because of missing decay scheme information. As we develop faster chemical procedures we should begin to acquire knowledge of new isotopes in this region. Some of our nuclide discoveries are detailed below.

^{87}Zr: In examining the yields of neutron deficient Zr isotopes, it became obvious that if the literature values for the γ-branches in ^{87}Zr were used, anomalous cross sections would result. Consequently we undertook a re-examination of ^{87}Zr decay. Table III lists the literature values for gamma abundances compared to our data which are based on growth of the ^{87}Y daughter. Table IV compares the ^{87}Zr half-life literature value with our observations. Figure 13 illustrates that our measurements of the absolute gamma intensities now also provide cross sections in excellent agreement with expectations.

^{84}Zr: The confirmation and characterization of the previously ill-defined isotope ^{84}Zr is complete. Observation of a prominent 112 keV gamma in a

zirconium sample was identified as belonging to ^{84}Zr via the growth and decay of ^{84}Y. The half-life we have observed is tabulated in Table V with previous reported half-lives. The absolute intensity of the 112 keV gamma branch, listed in Table VI, was obtained from the ^{84}Y activity. A suggested decay scheme is offered in Fig. 14. The cross section obtained using our half-life and branch intensity measurements is shown in Figs. 2-4 and its agreement with expectations is regarded as additional testimony to the validity of our results.

In 1976, it was reported[11] that a 4.6 sec isomeric state of ^{84}Y was discovered, but no measurable isomeric transition was observed. Our results are therefore indicative of decay to a level which is not that of the 4.6 sec isomer. A study of the report on 4.6 sec $^{84}Y^{m}$ reveals that the evidence for its assignment is particularly shaky.

"Applied" High-energy Spallation Reactions

High-energy spallation reactions with intense beams of light ions have been under discussion for a number of years as a possible means for converting non-fissile heavy elements into reactor fuel, thus augmenting the supply of fuel by a large factor.[12] We have directed our attention to applying the high beam intensity technology necessary for the accelerator-breeder program in another way. Namely, the spallation incineration of high-level nuclear waste. The concept is based on recognition that high-energy spallation of a traget produces a spectrum of radioactive residues lighter than the original system. This spectrum is dispersed about the stability line. If particularly egregious high-level nuclear wastes such as 29-yr ^{90}Sr or 30-yr ^{137}Cs serve as target, spallation incineration would be the breakdown of these materials into a mixture of short half-life, very long-lived

and stable products such that the degree of hazard will have been substantially reduced. We have been developing computer codes based on our results and expertise in spallation systematics. From a scientific perspective, such incineration looks promising. The technological and economic components of the issue are beyond our domain of competence.

As an example of the type of results we obtain,[13] Fig. 15 is the atomic percent composition of a thin target, initially pure ^{90}Sr, as a function of time during which a 250 mA beam of 800 Mev protons is run for thirty days followed by a cooling period. Only species with half-lives greater than several months are shown and the calculation has been run only through $\Delta A = 10$ because the program is still under development. The ^{90}Sr has been reduced by a factor of 50. The most hazardous component is ^{88}Y which, after 30 days bombardment has roughly 40% of the original activity. But the half-life of ^{88}Y is only 0.3 yrs and its activity dies in a manageable time.

Anomalous Relativistic Projectile Fragments in Emulsion Detectors

A very recent report[14] on the detection of "anomalous" nuclear matter produced from collisions of relativistic heavy ions with emulsion nuclei has attracted our attention and drawn upon our time. The phenomenon corresponds to the observation that fragments have mean free paths during their first few cms which are significantly shorter than normal and the only explanation which has not been ruled out is the hypothesized production of a percentage (6%) of species with a 2.5 cm mean free path corresponding to no conceivable nuclear species. Although this phenomenon has been in the cosmic ray literature on several occasions since 1954, it has not been until the availability of Bevlac beams that controlled experiments could be undertaken. The recent collaborative effort at Berkeley

has reduced several previous uncertainties considerably but still suffers from poor statistics. Nevertheless, there is no doubt that some effect is evident. We have undertaken a critical re-examination of more conventional explanations. We are admittedly out of our medium when discussing emulsion experiments, but our expertise in high-energy reactions has led us so far to three useful observations that lend themselves to the fragment enigma.

First, since our "soft spheres model" does such an excellent job in estimating nucleus-nucleus total reaction cross sections at high energies,[15] we proceeded to evaluate theoretical mean free paths in G5 emulsion. The accuracy of the soft spheres model is illustrated in Table VII taken from a recent Berkeley thesis on relativistic cosmic rays.[16] From the composition of G5 emulsion and the interaction cross sections of a RHI with each component, we calculate the mean free path of 2.1 GeV/A ^{16}O to be 10.30 cm. The literature values determined experimentally are 13.7, 12.6 and 13.0 cm, the latter being the recent determination by Heckman et al.[16] The difference is ascribable to the difficulty in detecting interactions with $\Delta Z = 0$ or 1, that is, the detection efficiency is less than unity. Heckman et al. estimated that ~16% of the total cross section was missed but it is apparent to us that ~30% is a more accurate estimate and that the detection efficiency of G5 for such interactions is closer to ~70%. For ^{4}He Heckman finds a mean free path of 21.8 cm compared to our calculated 18.6 cm. A measurement[18] of the $\Delta Z = 0$ reaction $^{1}H(^{4}He,^{3}He)pn$ at 6.85 GeV/c had a cross section of 24.1 mb which itself is ~23% of σ_R. The combination of $\Delta Z = 0$ and 1 must thus be much larger than the ~16% inferred by the Berkeley estimation procedure. For elementary singly-charged projectiles, the efficiency loss associated with $\Delta Z = 0$ and 1 should vanish. Indeed, we calculated for 2.1 GeV protons and 4.2 GeV π^- in G5, mean free paths of 31.9 cm and 36.8 cm respectively

compared to literature values of 33 $\pm$ 6 and 38.7 $\pm$ 3.5 respectively.[19]

Second, the recently published analysis[14] of mean free paths contained a parameterized Z dependence according to

$$\lambda(Z) = \Lambda(\text{beam})Z^{-b} \tag{9}$$

where Λ(beam) = 30.4 $\pm$ 1.6 and b = 0.44 $\pm$ 0.02. In this way, secondary fragments of any charge can be described by one function to improve statistics. The authors support this method by stating that Eq. (9) is consistent with our geometrical model. We fitted our calculated mean free paths for ^{4}He, ^{6}Li, ^{14}N, ^{16}O and ^{40}Ar to a power law and obtained

$$\lambda(Z) = 25.2\ Z^{-0.431} \tag{10}$$

The Z-dependence is in excellent agreement with Eq. (9) but the scaling factor Λ differs by ~21% from the experimental one, consistent with the underestimation of efficiency loss by the authors. However, the parametrization of λ should be with respect to A not Z! The experimental parameters are obtained from beam particles which are all stability valley occupants. But secondary fragments need not be and, in fact, are not confined thusly. Reaction cross sections are A-dependent and only very weakly Z-dependent. For instance, we calculated λ for ^{4}He to be 18.6 cm. Eq. (9) would imply λ for ^{6}He to be identical. To the contrary, we calculated λ for ^{6}He to be 13.9 cm!

Third, the analysis of the dependence of Λ on D, distance travelled in the emulsion seems to be based on Judek's 1972 two component expression[19]

$$\bar{\lambda}(D) = \frac{I_1 e^{-D/\lambda_1} + I_2 e^{-D/\lambda_2}}{I_1\left(\frac{1}{\lambda_1}\right)e^{-D/\lambda_1} + I_2\left(\frac{1}{\lambda_2}\right)e^{-D/\lambda_2}}$$

where I_1 is the fraction of beam which is of type one with $\lambda = \lambda_1$. The experiment though, involves analyzing tracks within segments of lengths Δx lying anywhere between 1.0 and 20.0 cm. The above expression is an approximation to the true expression when $\Delta x/\lambda \ll 1$ which is not, however, the case. We have derived the exact expression which is

$$\bar{\lambda}(D,\Delta x) = \frac{I_1 e^{-D/\lambda_1}(1-e^{-\Delta x/\lambda_1}) + I_2 e^{-D/\lambda_2}(1-e^{-\Delta x/\lambda_2})}{I_1\left(\frac{1}{\lambda_1}\right)e^{-D/\lambda_1}(1-e^{-\Delta x/\lambda_1}) + I_2\left(\frac{1}{\lambda_2}\right)e^{-D/\lambda_2}(1-e^{-\Delta x/\lambda_2})}$$

We have done only a limited amount of space searching on I_1, I_2, λ_1 and λ_2 but show in Fig. 15 the fit calculated with $I_1 = 90\%$, $\lambda_1 = 10.3$ (2.1 GeV/A normal ^{16}O) and $I_2 = 10\%$, $\lambda_2 = 3.8$ (anomalous component). The agreement with the data is reasonable and corresponds to $A \sim 190$, not the $Z \sim 300$ alluded to in the recent report. Our examination of the phenomenon will continue but much better statistical data are needed.

References

(1) G. Rudstam, Z. Naturforschg. 21a, 1027 (1966).

(2) N. T. Porile, Phys. Rev. C19, 2288 (1979).

(3) J. B. Cumming et al., Phys. Rev. C10, 739 (1974).

(4) T. H. Ku and P. J. Karol, Phys Rev. C16, 1984 (1977).

(5) W. D. Myers, "Droplet Model of Atomic Nuclei," Plenum, NY.

(6) S. B. Kaufman and E. P. Steinberg, Phys. Rev. C72, 167 (1980).

(7) K. J. LeConteur, "The Statistical Model" in Nuclear Reactions, Vol. I, P. Endt, ed.

(8) Reference 6 and private communication, 1980.

(9) C. M. Lederer and V. S. Shirley, "Table of Isotopes" 7th ed, John Wiley, NY (1978).

(10) P. E. Haustein et al., Atomic Masses and Fundamental Constants 6, 475 (1980).

(11) R. Iafigliola and J. K. P. Lee, Phys. Rev. C13, 2075 (1976).

(12) Proc. Info. Mtg. on Accelerator-Breeding, BNL, 1977 (Conf-770107, unpublished).

(13) P. Karol, "Intermediate Energy Spallation and the Transmutation of Long-lived Radioisotopes" (in press, Proc. Intl. Conf. Nucl. Waste Transmutation, Austin, TX 1980).

(14) E. W. Friedlander et al., LBL-11136 (1980) in press.

(15) P. J. Karol, Phys. Rev. 11C, 1203 (1975).

(16) L. Wilson, Ph.D. Thesis, LBL-7723 (1978) unpublished.

(17) H. Heckman et al., Phys. Rev. C17, 1735 (1978).

(18) G. Bizard et al., Nucl. Phys. A285, 461 (1977).

(19) B. Judek, Can. J. Phys. 50, 2082 (1972).

(20) B. Judek, Proc. XIV Intl. Cosmic Ray Conf. 7, 2349 (1975).

Table I. Thermometric Slopes in Exponential Regions of Spallation Mass Yield Curves

Projectile	Energy (lab)	Target	Slope (% per amu)	Rudstam's P
π	190 MeV	89Y	18	34.8* 23.8**
^{1}H	800 MeV	89Y	9.5	12.9
^{4}He	720 MeV	89Y	13	13.9
^{1}H	800 MeV	^{100}Mo	11.8	12.9

*Without and **with pion rest mass energy

Table II. Relative Spallation Cross Sections from 800 MeV Protons Incident on ^{130}Te

Isotope	Half-life	Relative σ
^{129}Te	70 m	21.0
^{129}Sb	4.4 h	10.0
^{128}Sb	9.1 h	3.9
^{127}Sb	3.9 d	12.4
^{124}I	4.2 d	4.4
^{122}Sb	2.7 d	11.4
^{121}I	2.1 h	0.63
$^{120}Sb^{m}$	5.8 d	5.1
$^{119}Te^{m}$	4.7 d	2.6
$^{119}Te^{g}$	16 h	2.5
$^{118}Sb^{m}$	5.0 h	6.7
^{117}Te	64 m	2.2
^{117}Sb	2.8 h	11.3
$^{117}In^{m}$	1.9 h	3.0
$^{117}In^{g}$	44 m	3.3
^{115}Sb	32 m	5.0
^{112}Ag	3.1 h	3.3
^{111}In	2.8 d	11.4
$^{111}Cd^{m}$	49 m	5.5
^{110}Sn	4.0 h	1.8
^{109}In	4.2 h	5.3
$^{104}Ag^{g}$	69 m	4.8
^{103}Ag	1.1 h	1.8
^{100}Rh	21 h	3.2
^{97}Ru	2.89 d	2.5
^{96}Tc	4.4 d	2.9
^{95}Tc	20 h	2.0
^{95}Ru	1.7 h	0.6
^{94}Tc	4.9 h	1.6
$^{93}Mo^{m}$	7.0 h	1.7
$^{87}Y^{m}$	13.2 h	0.9

Table III. Gamma Intensities for 1.7h-^{87}Zr

Gamma Energy (keV)	Table of Isotopes	This Work*
1210	.013	.00916 ± .00028
1228	.04	.0278 ± .0005

*weighted means of four determinations

Table IV. ^{87}Zr Half-Life

	Ref.	This Work*
1.60 h	PR 178 1732 (69)	1.693 ± 0.017 h
1.57 h	JINC 25 151 (63)	

*weighted mean of four determinations

Table V. ^{84}Zr Half-Life

$t_{1/2}$	Ref.	This Work*
28.5 m (unassigned)	NP A161 12 (71)	
5.0 m	JINC 33 3223 (71)	25.7 ± 0.5 m
16 m	Yad F 1 385 (65)	

*weighted mean of seven determinations

Table VI. Intensity of 112-keV Gamma in ^{84}Zr*

Sample	Target	I (%)
60	^{92}Mo	97.8 ± 8.1
63	"	106.0 ± 9.1
69	"	96.6 ± 7.1
66	^{96}Mo	91.7 ± 20.9
68	^{100}Mo	82.8 + 23.1
weighted average		98.4 ± 4.4

*using 56.8% 1040-keV branch of 40m-^{84}Y

Table VII. Comparison of Nucleus-Nucleus Reaction Cross Sections with the Soft Spheres Model*

Reaction	Kinetic Energy (GeV/A)	Experiment (mb)	Soft Spheres (mb)
C-H	2.1	270 ± 14	266
C-H	0.87	260 ± 14	264
He-H	2.1	111 ± 6	106
He-H	0.87	120 ± 6	105
D-H	2.1	60 ± 16	72.5
C-D	2.1	426 ± 15	469
C-D	0.87	411 ± 21	466
He-D	2.1	203 ± 8	218
He-D	0.87	198 ± 10	216
D-D	2.1	134 ± 8	141.3
C-He	2.1	535 ± 19	549
C-He	0.87	527 ± 20	547
He-He	2.1	276 ± 14	269
He-He	0.87	262 ± 18	268
C-C	2.1	888 ± 44	954
C-C	0.87	939 ± 50	951

*Ref. 16

FIGURE CAPTIONS

Figure 1. Mass defects for A=100 in the region near stability showing symmetric parabolic behavior with Z as abscissa and asymmetry with N/Z as abscissa.

Figure 2. Relative isobaric yield curve, mass adjustments included, for Zr isotopes from 500 MeV protons bombarding ^{89}Y.

Figure 3. Same as Figure 2 but for Y and Zr isotopes from ^{92}Mo.

Figure 4. Same as Figure 3 but for ^{96}Mo.

Figure 5. Same as Figure 3 but for ^{100}Mo.

Figure 6. Relative isobaric yield curve, mass adjustments included, for As and Ge isotopes from 800 MeV protons bombarding ^{89}Y.

Figure 7. Same as Figure 6, but for ^{100}Mo.

Figure 8. Relative mass-yield curve for 800 MeV proton induced spallation of ^{100}Mo.

Figure 9. Relative isobaric yields of Zr isotopes from various targets at 800 MeV (open circles) and 500 MeV (closed circles) showing lack of bombardment energy dependence.

Figure 10. INC calculation for 1 GeV protons on ^{197}Au to produce cascades of $\Delta A = 15$ (open circles) and $\Delta A = 16$ (closed circles) showing correlation between average deposition energy and cascade path as qualified by product N/Z.

Figure 11. Average deposition energy per cascade as a function of initial impact parameter.

Figure 12. Average deposition energy per cascade as a function of cascade length, ΔA.

Figure 13. Relative isobaric yield curves for production of Zr isotopes from various targets using decay data in Table III for ^{87}Zr. Black squares for ^{87}Zr are what is obtained using Table of Isotopes data.

Figure 14. Decay scheme of 26m ^{84}Zr.

Figure 15. Change in composition of an initially pure ^{90}Sr sample as a function of time due to high intensity spallation transmutation.

Figure 16. Data and analysis from reference 14 on the anomalous mean free paths of secondary relativistic fragments. Heavy histogram is our fit.

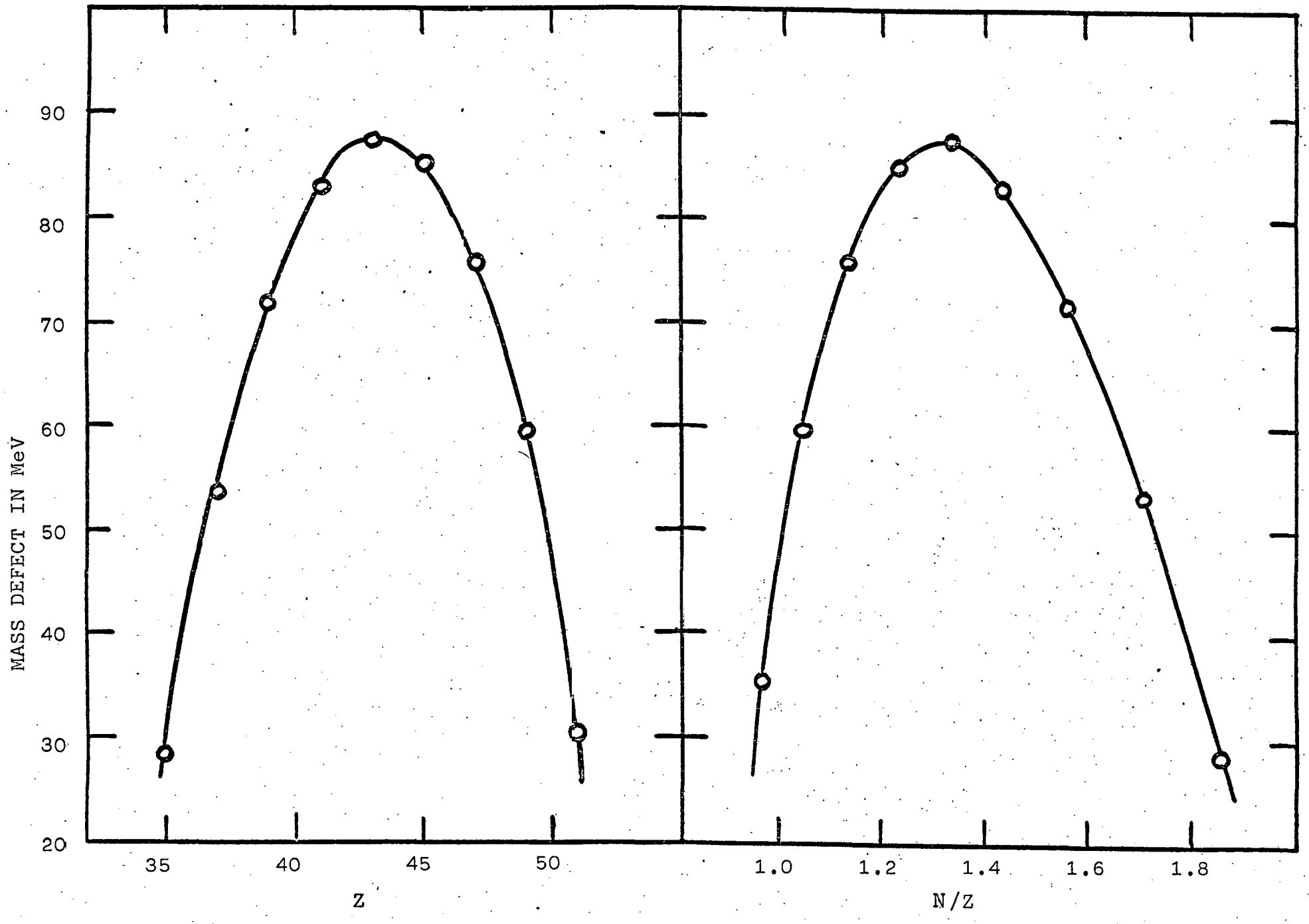
MASS DEFECT IN MeV
90
80
70
60
50
40
30
20
35
40
45
50
Z
1.0
1.2
1.4
1.6
1.8
N/Z

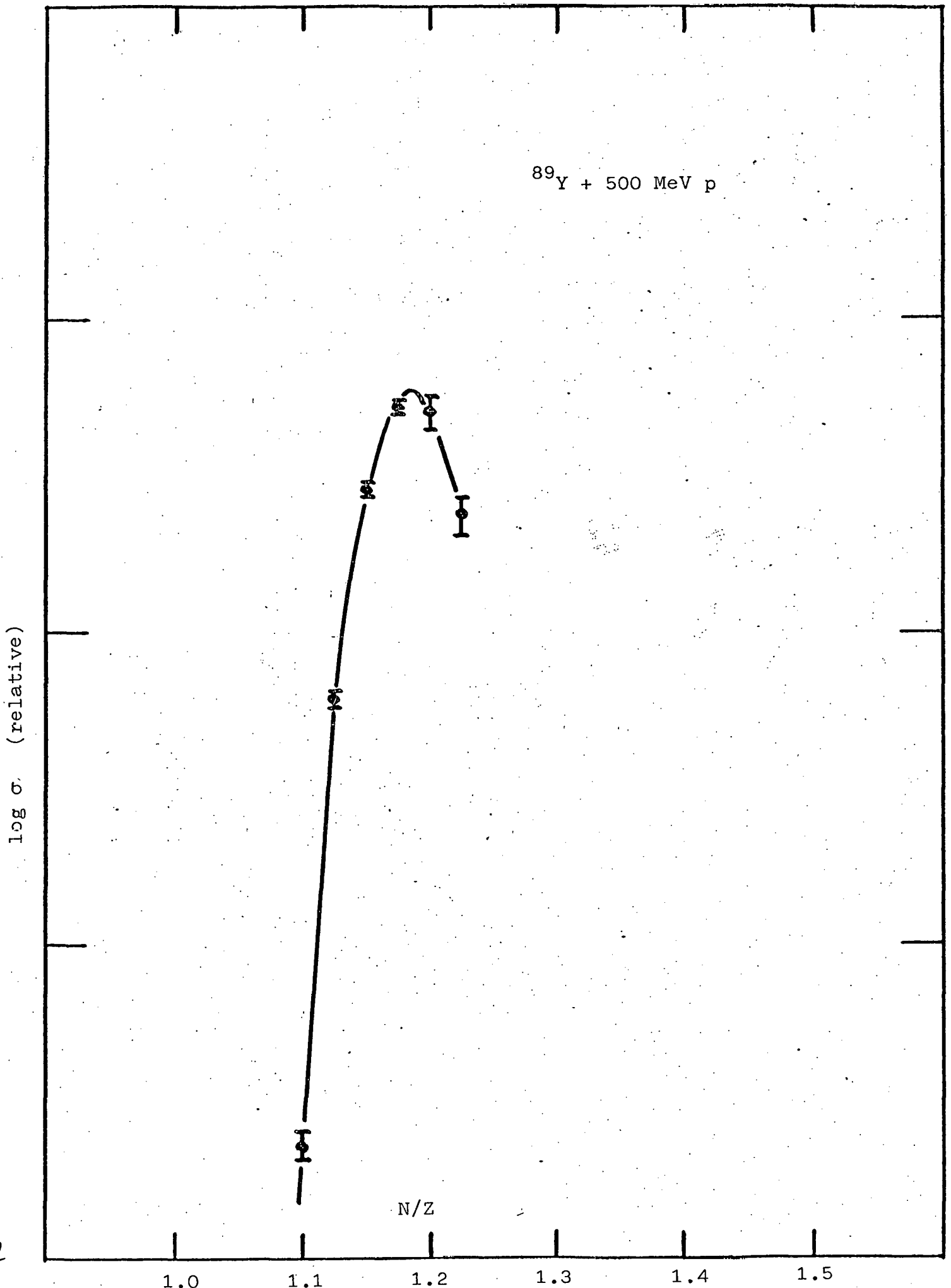
^{89}Y + 500 MeV p
log σ (relative)
N/Z
1.0
1.1
1.2
1.3
1.4
1.5

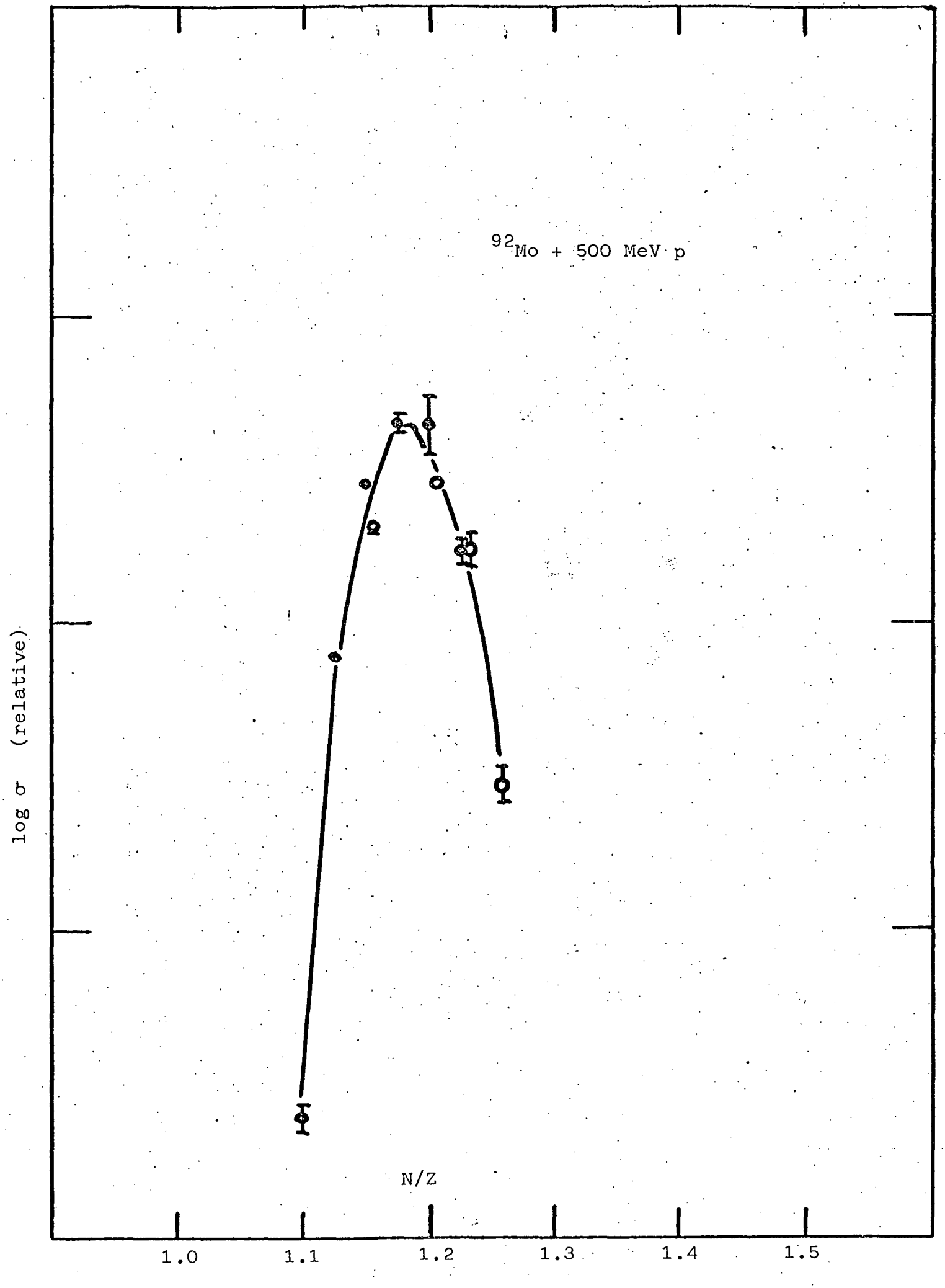
^{92}Mo + 500 MeV p
log σ (relative)
N/Z
1.0
1.1
1.2
1.3
1.4
1.5

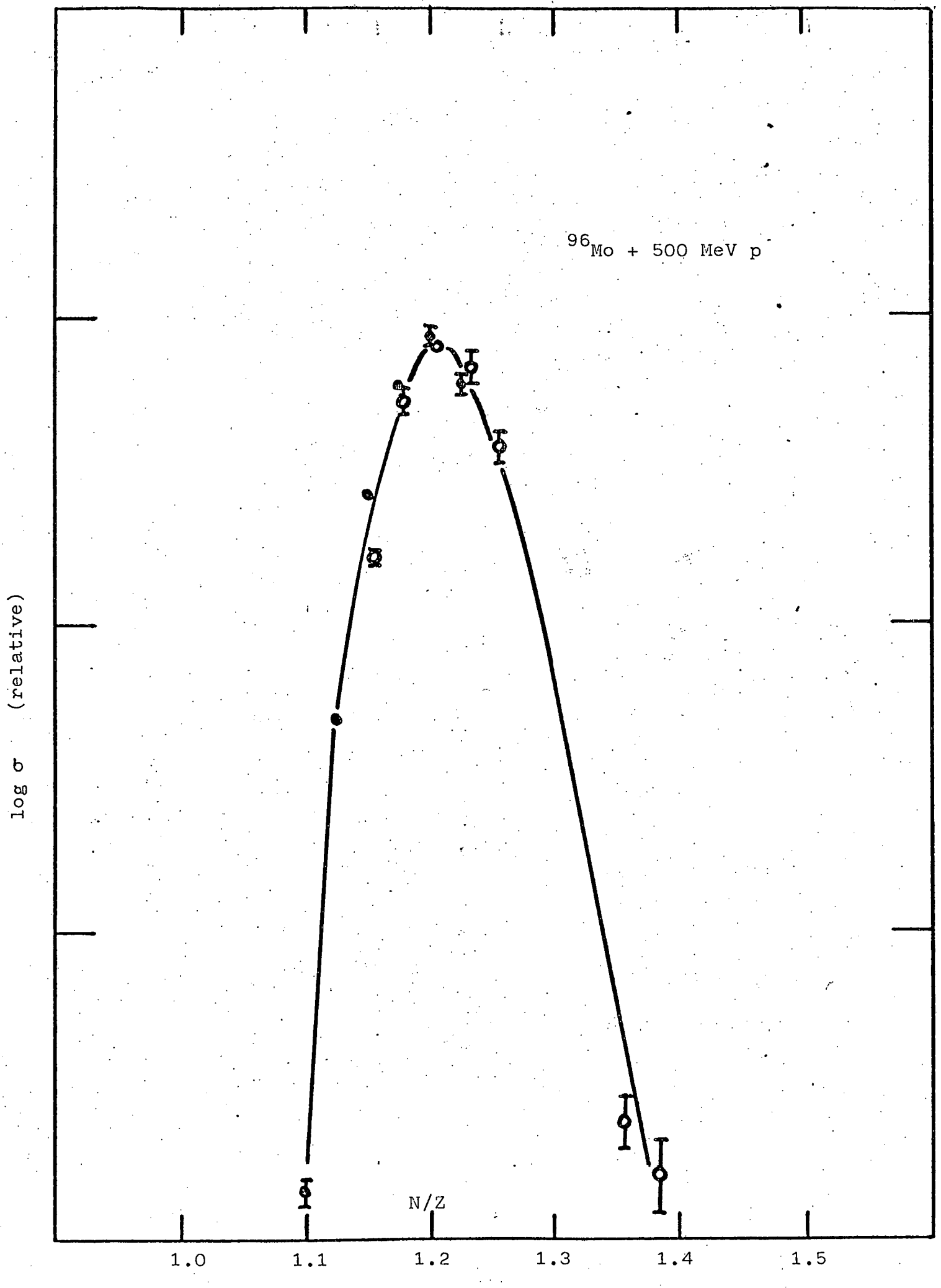
^{96}Mo + 500 MeV p
log σ (relative)
N/Z
1.0
1.1
1.2
1.3
1.4
1.5

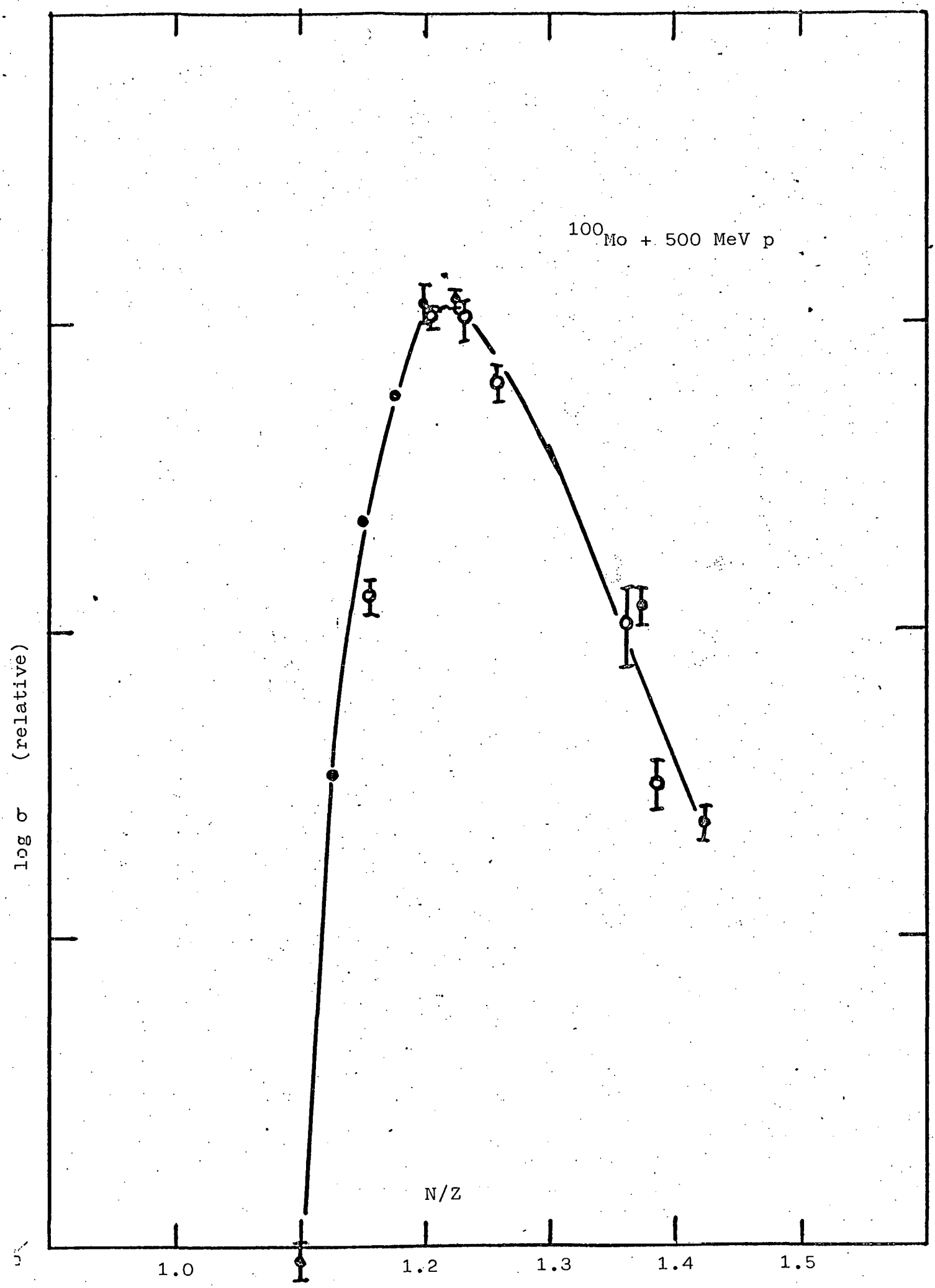
^{100}Mo + 500 MeV p
log σ (relative)
N/Z
1.0
1.2
1.3
1.4
1.5

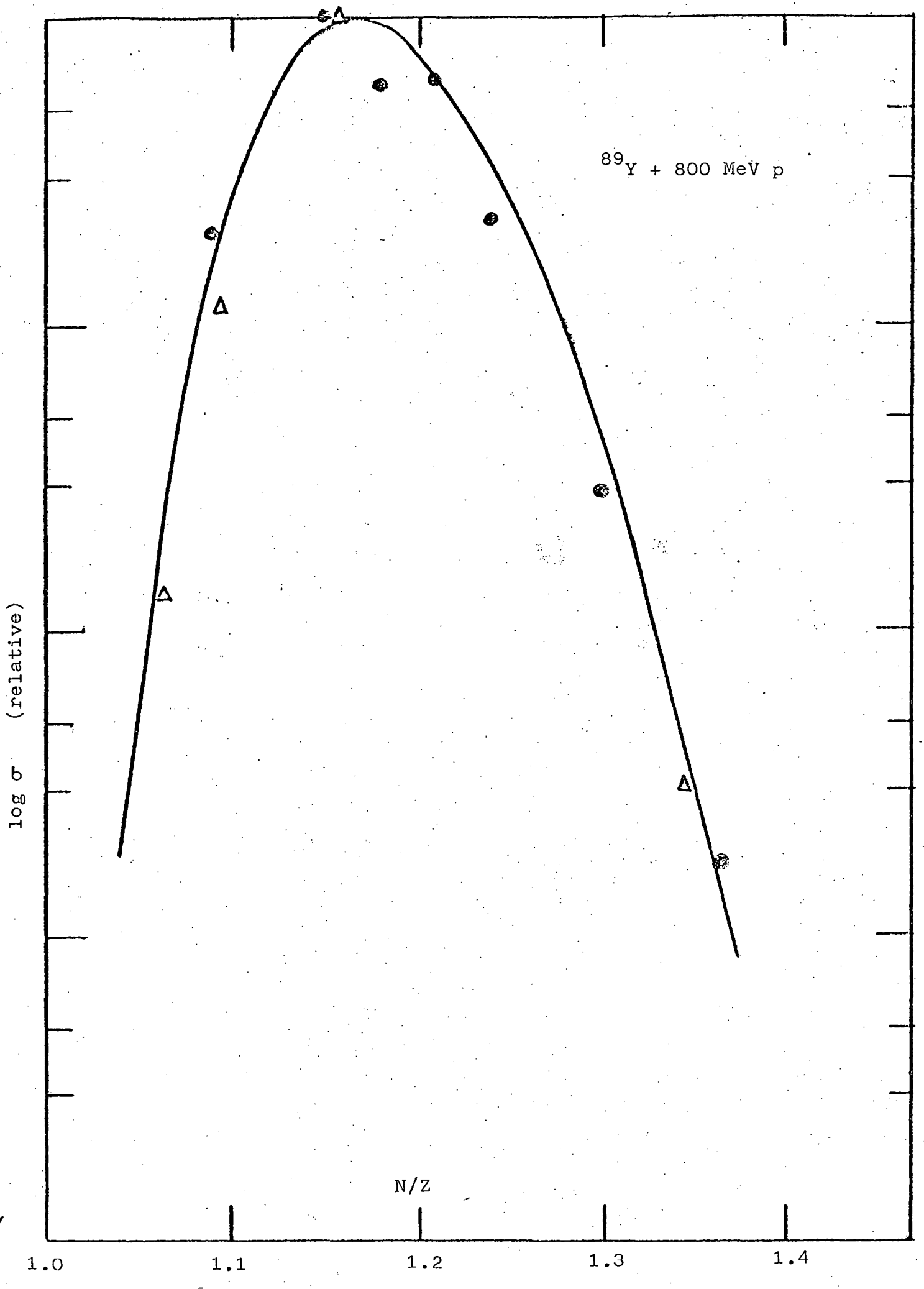
^{89}Y + 800 MeV p
log σ (relative)
N/Z
1.0
1.1
1.2
1.3
1.4

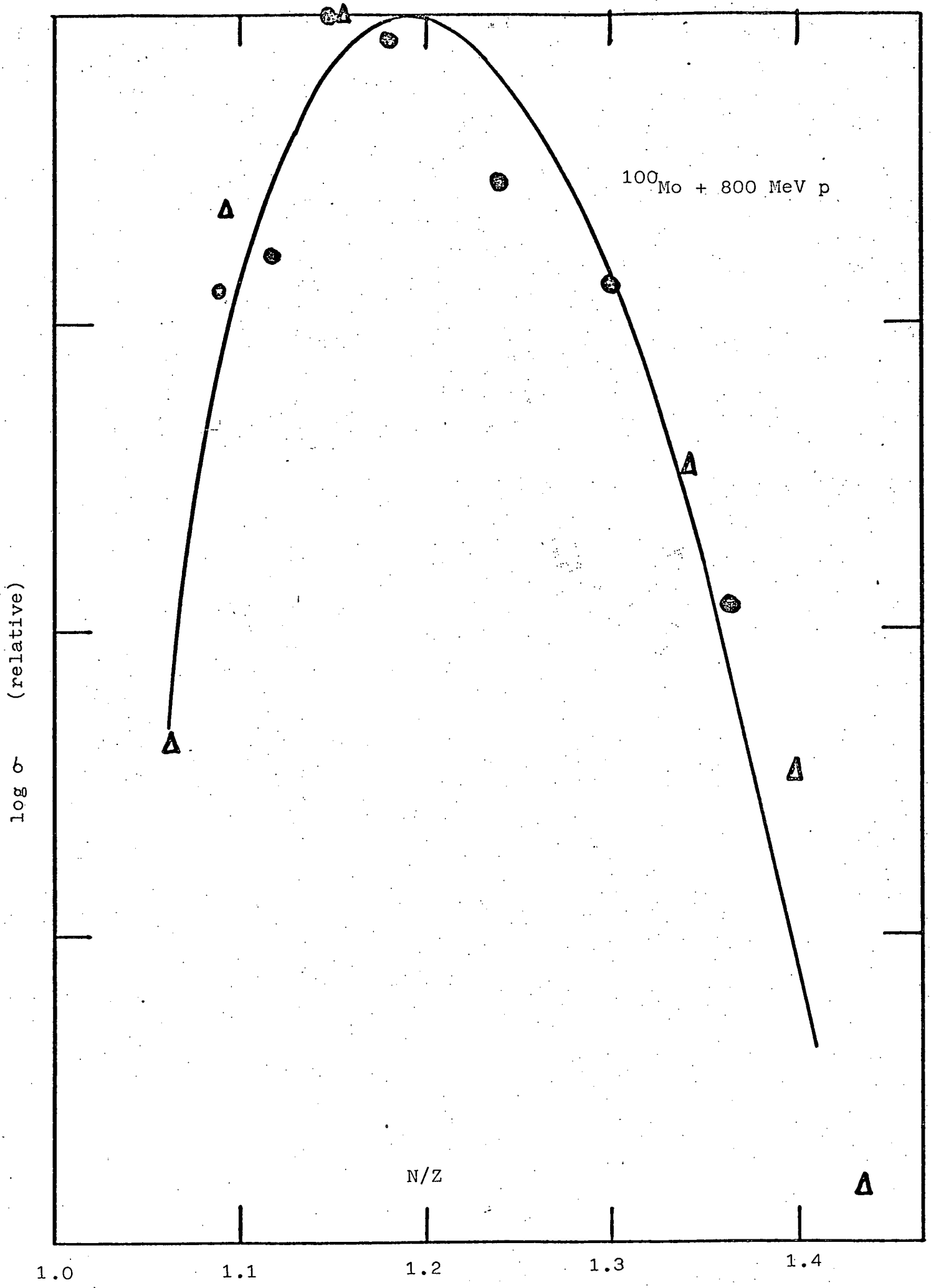
^{100}Mo + 800 MeV p
log σ (relative)
N/Z
1.0
1.1
1.2
1.3
1.4

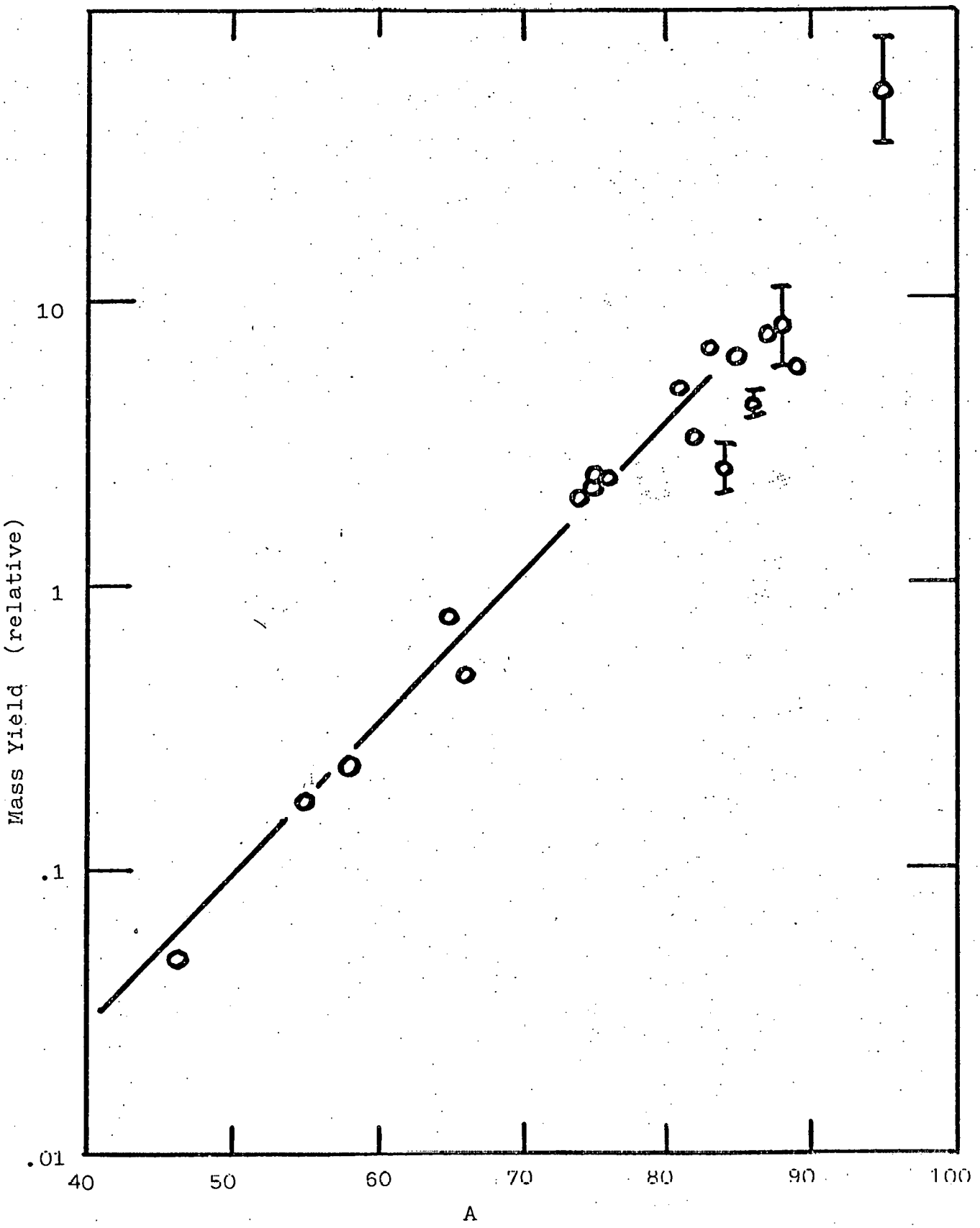
Mass Yield (relative)
10
1
.1
.01
40
50
60
70
80
90
100
A

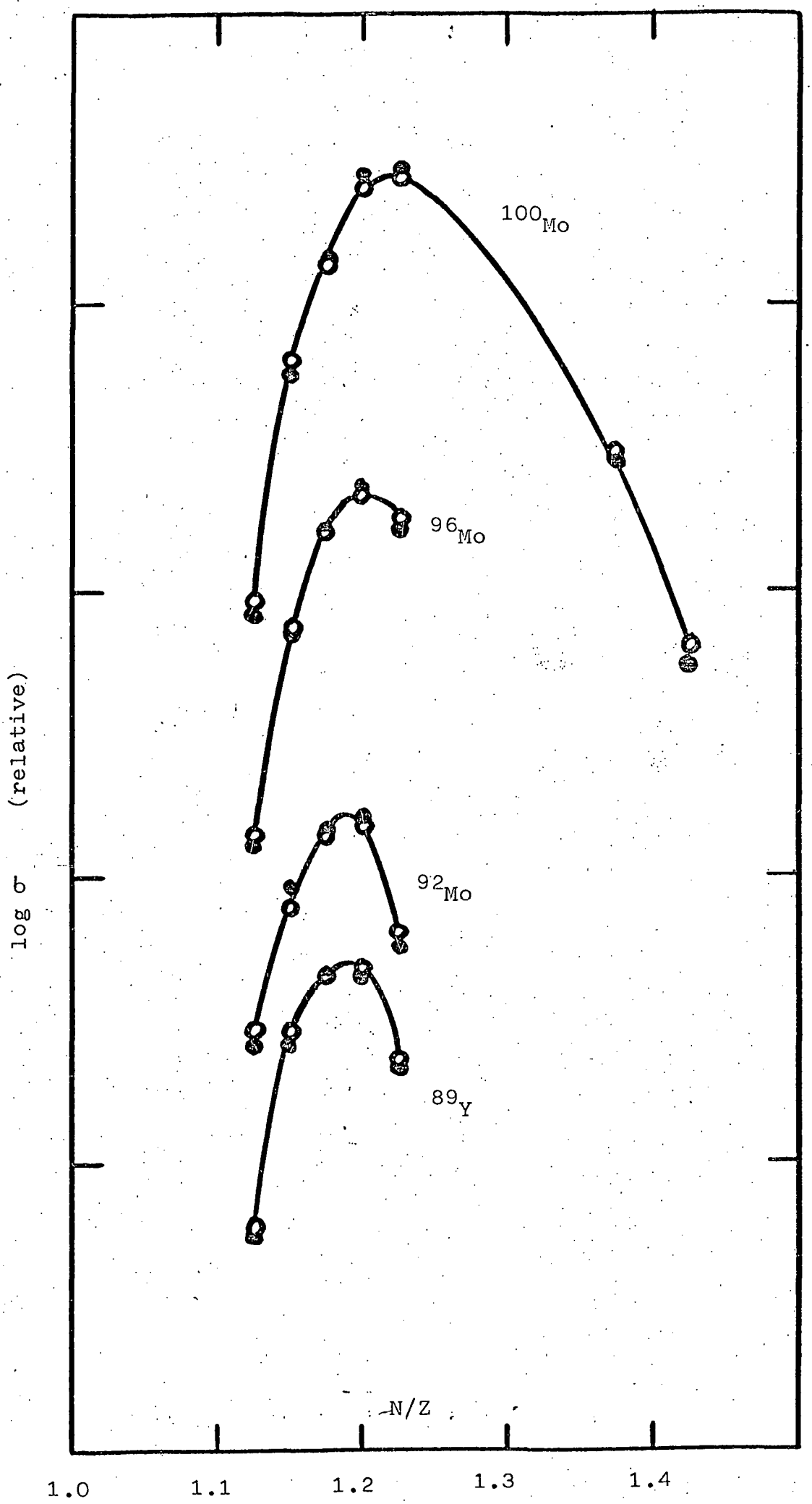
100Mo
96Mo
92Mo
89Y
log σ (relative)
N/Z
1.0
1.1
1.2
1.3
1.4

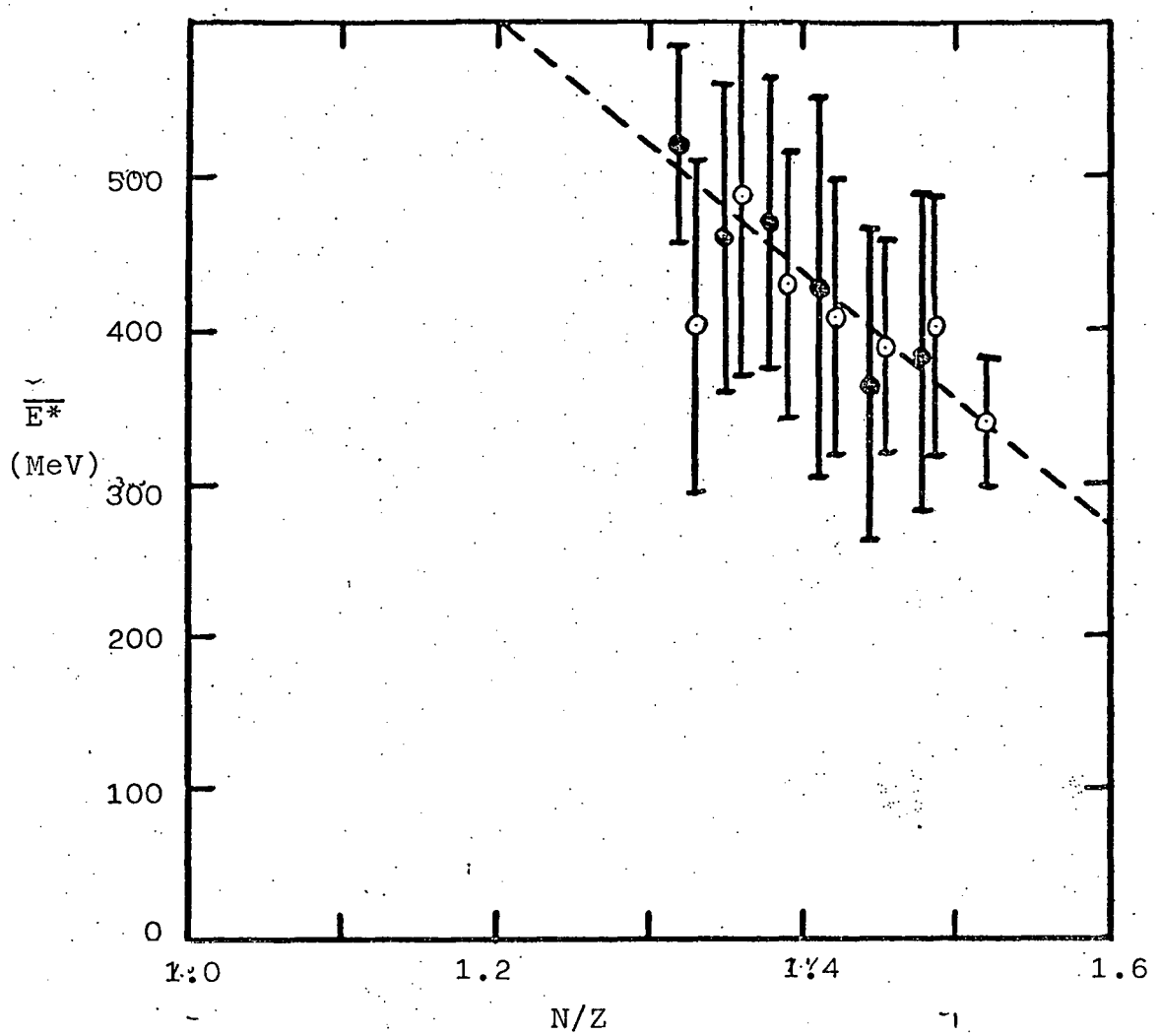
500
400
$\widetilde{E^*}$
(MeV)
300
200
100
0
1.0
1.2
1.4
1.6
N/Z

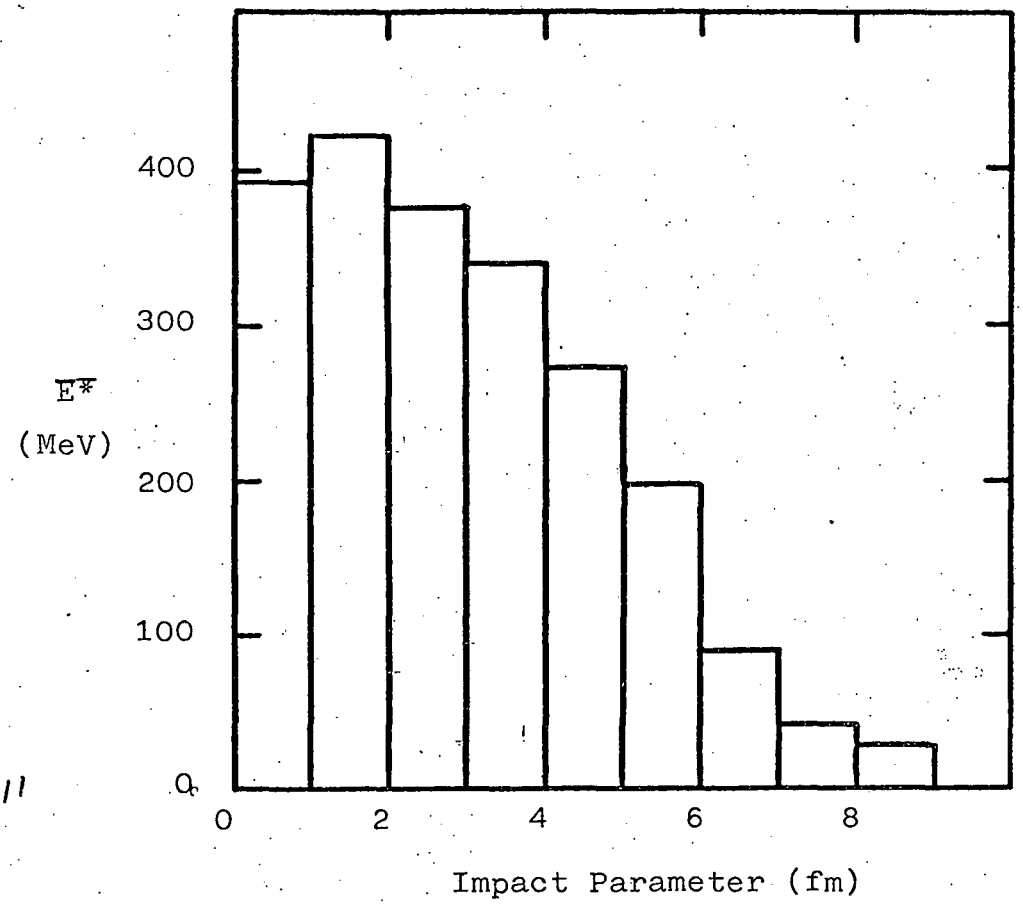
400
300
E*
(MeV)
200
100
0
0
2
4
6
8
Impact Parameter (fm)

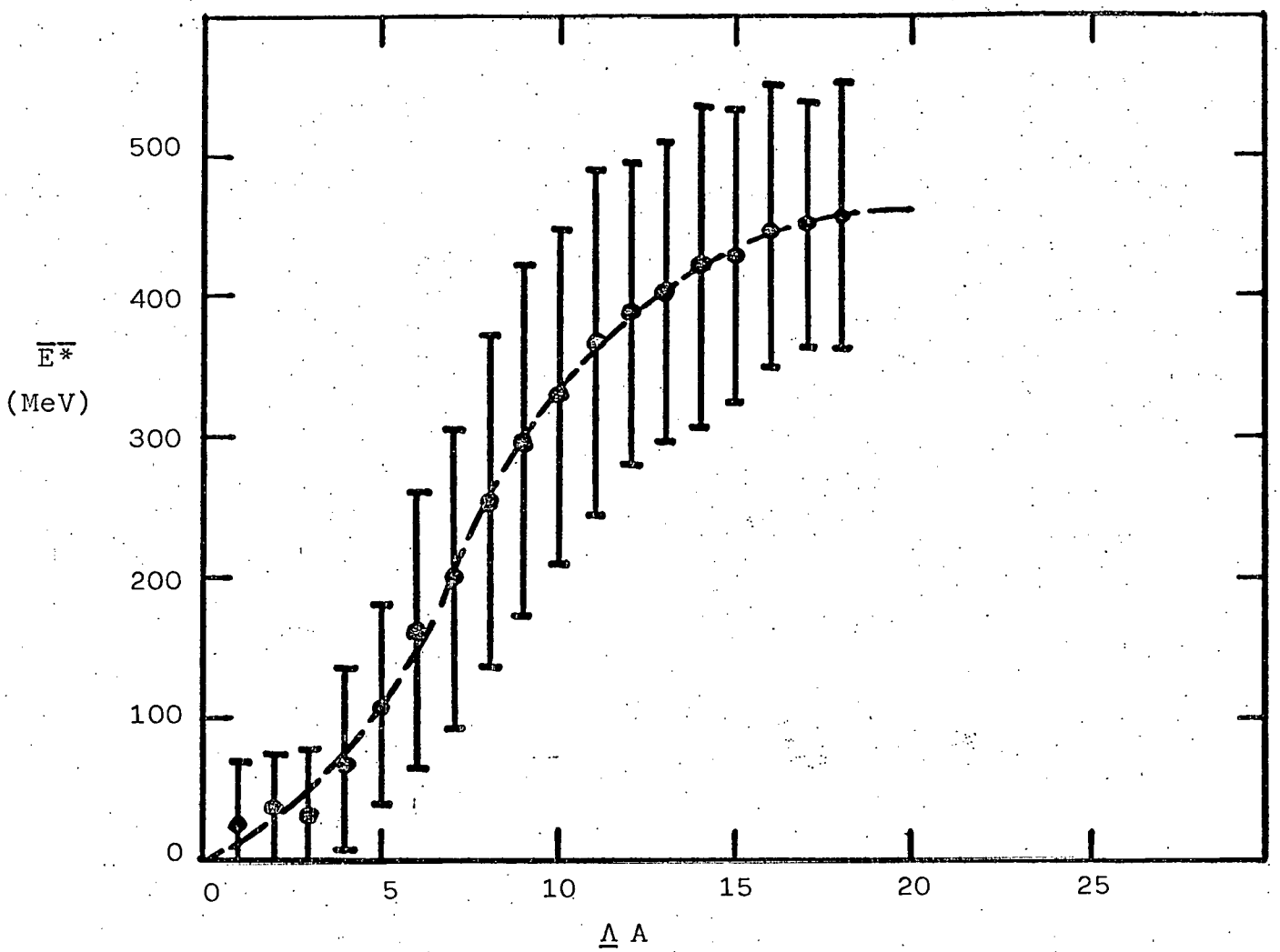
$\overline{E^*}$
(MeV)
500
400
300
200
100
0
0
5
10
15
20
25
$\underline{\Lambda}$ A

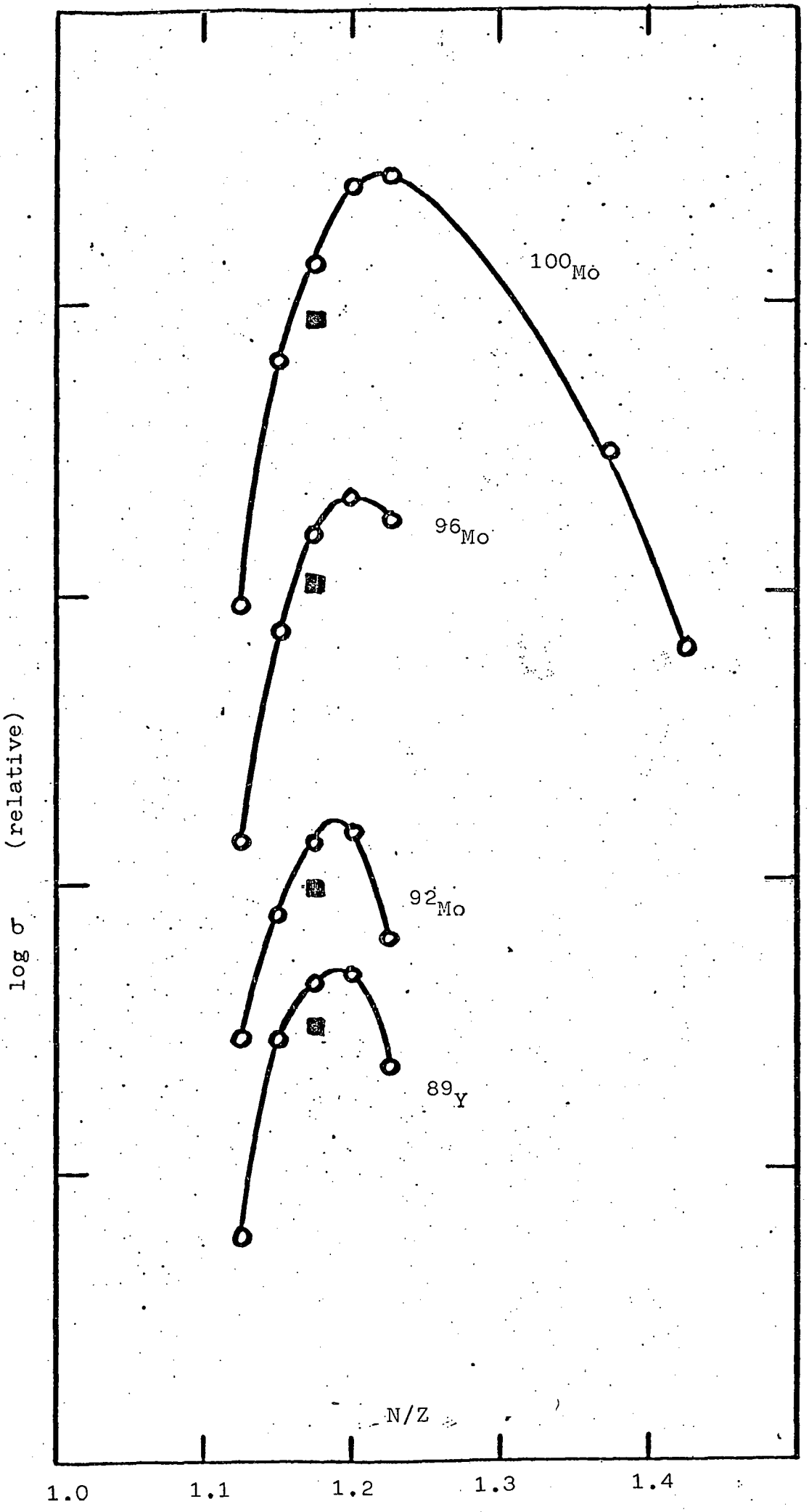
log σ (relative)
100Mo
96Mo
92Mo
89Y
N/Z
1.0
1.1
1.2
1.3
1.4

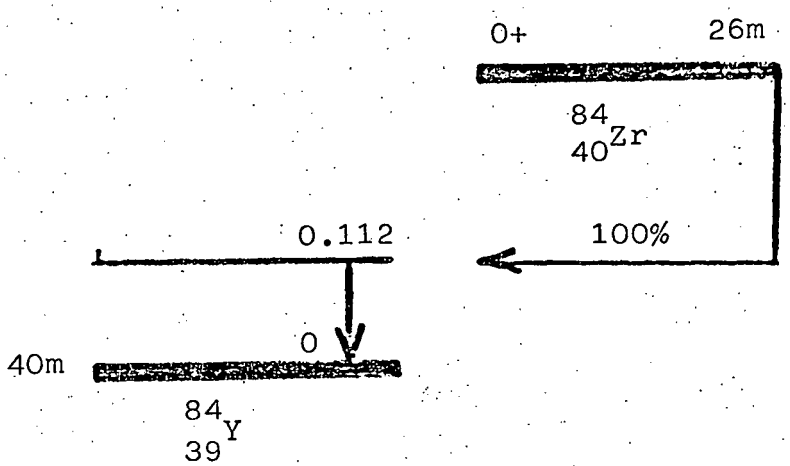
0+
26m
84
40Zr
100%
0.112
0
40m
84
39Y

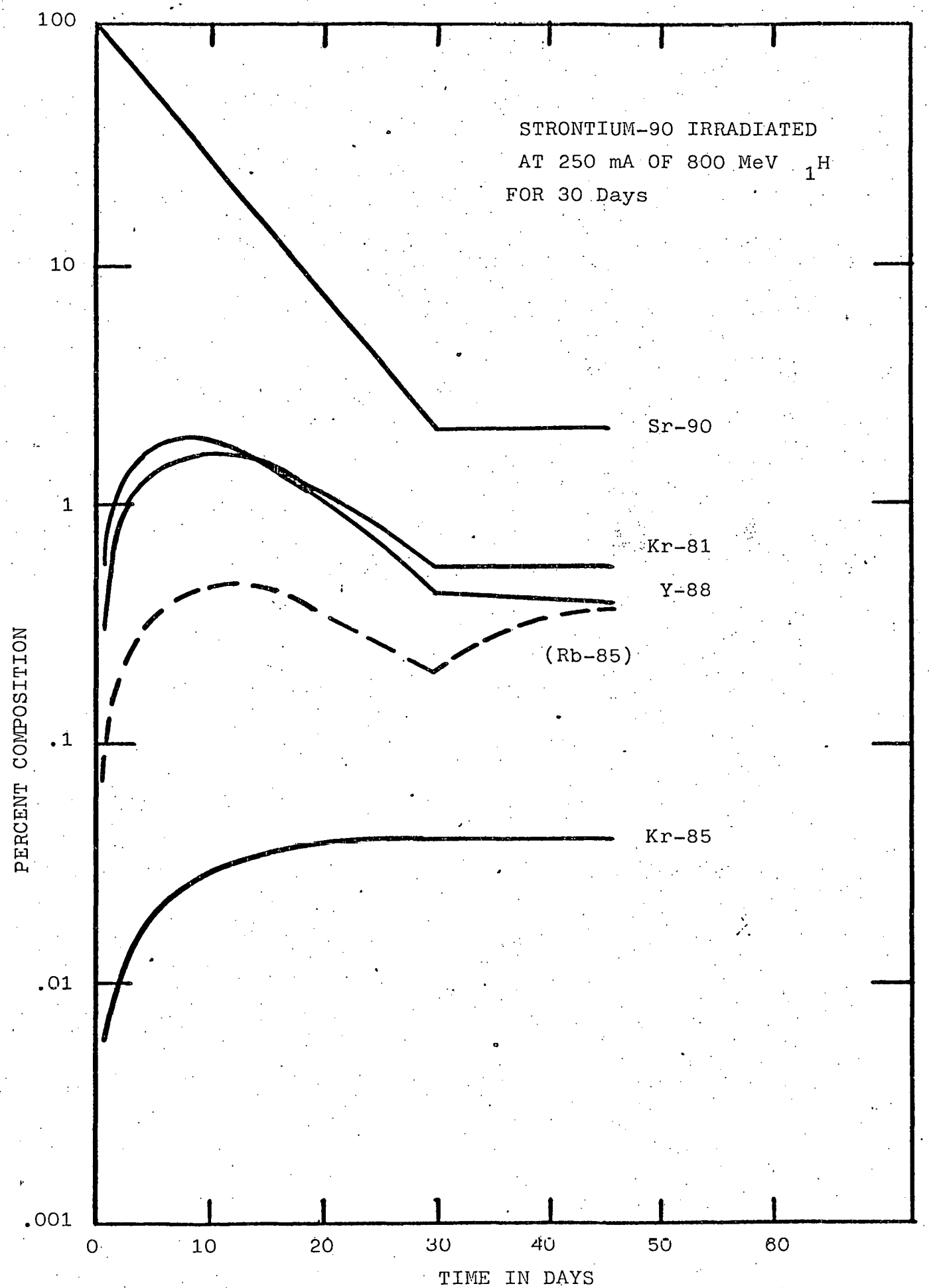
STRONTIUM-90 IRRADIATED
AT 250 mA OF 800 MeV $_1^1H$
FOR 30 Days
Sr-90
Kr-81
Y-88
(Rb-85)
Kr-85
PERCENT COMPOSITION
100
10
1
.1
.01
.001
0
10
20
30
40
50
60
TIME IN DAYS

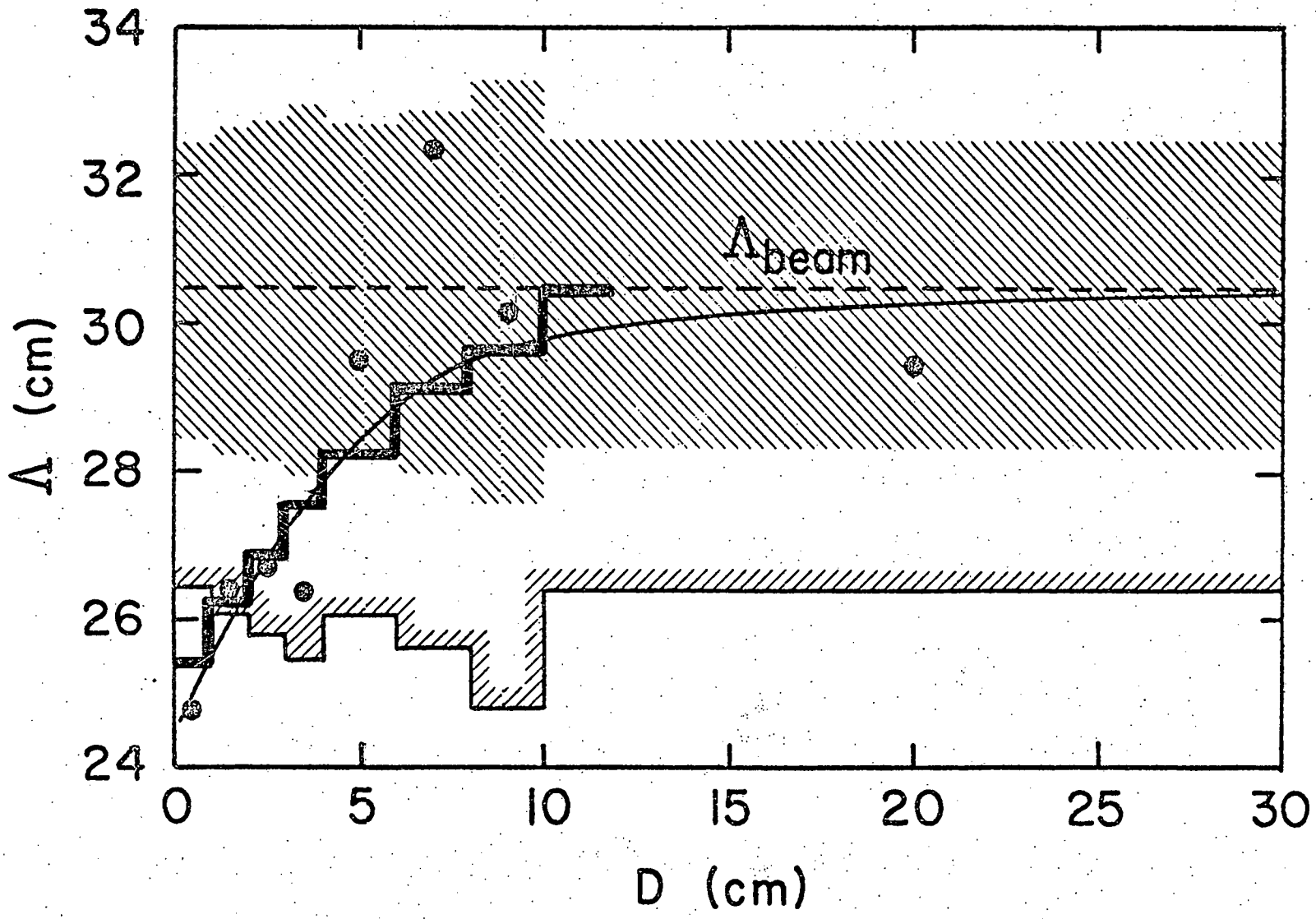

Fig. 16

Personnel (1980)

Paul J. Karol, Associate Professor of Chemistry, Carnegie-Mellon University, Principal Investigator.

Dr. Seiichi Shibata, Postdoctoral Research Associate, on leave from the Tokyo Institute for Nuclear Research.

Mr. Michael Tobin, graduate research assistant, B.S. in Chemistry from the University of Pittsburgh, 1979.

Mr. Ford Stoll, graduate part-time research assistant, summer 1980, equipment repair and data analysis.

Mr. Dewayne Anderson, undergraduate chemical engineering major, part-time assistant, data analysis.

Mr. Robert Dragos, undergraduate chemical engineering major has been doing his senior research on the nuclear waste project at no cost to this contract.

Reports, Publications and Presentations

P. J. Karol, Relevance of Final State Nucleon-Nucleon Charge Exchange in Inclusive ($\pi,\pi N$) Reactions, Phys. Rev. C (in press).

P. J. Karol, Transmutation of Long-lived Radioisotopes by Intermediate Energy Spallation, Proc. Int'l Conf. on Nuclear Waste Transmutation, Austin, Texas, July 22-24, 1980 (in press).

P. J. Karol, S. Shibata and M. Tobin, Deep Spallation with Intermediate Energy Projectiles, Workshop on Intermediate Energy Nuclear Chemistry, Los Alamos, New Mexico, June 1980 (COO-4721-3).

B. J. Dropesky and P. J. Karol, Proceedings of the Workshop on Intermediate Energy Nuclear Chemistry, Los Alamos, New Mexico, June 1980 (in press).

P. J. Karol, Nuclear Transparency at Intermediate Energies, (in revision).

S. Shibata and P. J. Karol, Decay of 26-minute Zr-84, (in preparation).

S. Shibata and P. J. Karol, Gamma-ray Abundances of 1.7 hr Zr-87, (in preparation).

P. J. Karol, Experimental Nuclear and Radiochemistry Progress Report, 1979 (COO-4721-2).

34C